Re-submitted to: Materials Science and Engineering B (**MSB-D-13-00826**)

Date: October 18, 2013

Photocatalytic hydrogen generation with simultaneous organic degradation by a visible light-driven CdS/ZnS film catalyst

Xi Wang[1,2] and Xiao-yan Li[2]*

[1] School of Chemistry and Environment, South China Normal University, Guangzhou, Guangdong, China

[2] Environmental Engineering Research Centre, Department of Civil Engineering, The University of Hong Kong, Pokfulam Road, Hong Kong

(*Corresponding author: phone: 852 2859-2659; fax: 852 2859-5337; e-mail: xlia@hkucc.hku.hk)

Abstract

A layered CdS/ZnS catalyst film was synthesized on glass using the stepped chemical bath deposition method. The film catalyst was shown as visible light-driven photocatalyst capable of producing H_2 under visible light. The ZnS outer layer helped suppress the recombination of photo-generated electron-hole pairs on the CdS base layer, leading to faster H_2 generation. The use of the ZnS layer also greatly improved the stability of the catalyst film and prevented the leaching of Cd^{2+} from the CdS layer. Deposition of Ru on the catalyst film further increased its photoreactivity for H_2 production. The photocatalyst was effective in H_2 production together with the degradation of model organic substances, such as formic acid, methanol, and ethanol. The greatest H_2 production rates were achieved

using the CdS/ZnS/Ru film in the formic acid solution at 123 μmol/m^2-h under visible light and 135 mmol/m^2-h under the simulated solar light. The corresponding theoretical reduction rates of chemical oxygen demand (COD) were 1.9 and 2.1 g/m^2-h, respectively. As the multilayer CdS/ZnS/Ru film catalyst can be easily separated from water, it has a great potential for simultaneous photocatalytic hydrogen generation and organic wastewater treatment using solar energy.

Keywords: CdS-ZnS, hydrogen generation, organic degradation, photolysis, photocatalyst film, solar energy.

1. Introduction

Hydrogen is one of the most promising forms of clean and renewable energy. Photocatalytic hydrogen generation from water is an attractive and environmentally friendly method to harvest solar energy [1, 2]. However, while visible light (λ>420 nm) covers a large portion of the solar spectrum, most photocatalysts, such as TiO_2, function only under energy-intensive ultraviolet (UV) irradiation. Efforts have been made in recent years to develop photocatalysts, such as metal oxides (e.g. ZnO) and metal sulfides (e.g. CdS), that respond to both UV and visible lights for water photolysis [3]. However, most photocatalysts are still hampered by typical problems such as the recombination of photo-generated electron-hole pairs [4] and low stability of the catalysts due to photo-corrosion [5-7].

In addition to hydrogen evolution (H^+ reduction), photocatalytic reactions in water possess a strong oxidation power that may be utilized for pollutant degradation [8, 9]. During the photocatalytic process under solar light, pollutants such as sulfide and organic matters[3, 10], including alcohols [11-15] and organic acids [6, 15, 16], can function as electron donors for hydrogen evolution, while the pollutants are degraded. In such a

photocatalytic application, the purposes of both hydrogen generation and wastewater treatment using solar energy can be achieved [6, 9].

Most visible light-driven photocatalysts are produced and applied in a powder form. However, for potential application in wastewater treatment, an easy separation of the photocatalysts from the treated effluent is required. Hence, there are efforts made to immobilize photocatalysts in solid carriers to eliminate the need for separation in the treatment process [17-20]. However, few studies have been conducted on the use of film-type catalysts for photocatalytic hydrogen production together with organic pollutant degradation [21-23]. In our previous study, composite CdS/ZnS nanoparticles were synthesized as a visible light-driven photocatalyst for H_2 production [24]. The present work aims to develop a multilayer film-type CdS/ZnS catalyst that can achieve both photocatalytic H_2 production and organic degradation under the simulated solar light or visible light.

2. Materials and Methods

2.1 Preparation of the CdS/ZnS thin film catalysts

Microscopic glass slides were used as the base material for the deposition of the CdS/ZnS catalyst films. The catalyst was deposited on both sides of a slide with a dimension of 2.5 × 5.5 cm^2. The glass slides were cleaned thoroughly with detergent, degreased with ethanol in an ultrasonic cleaner, and then etched in 4% HNO_3 solution. The chemical bath deposition (CBD) process was used to deposit the catalyst material on the glass surface. The CdS coating solution was prepared using an aqueous solution of 0.005 M $Cd(NO_3)_2$ in a 0.005 M NH_4NO_3 buffer mixed with 0.06 M thiourea ($SC(NH_2)_2$). The pH of the coating solution was adjusted to 8.5-9.5 using 25% NH_4OH. During the deposition process, the glass slides were immersed in the coating solution in a beaker, which was then placed in a water bath heated to 50 °C. The CBD process lasted for 30 min to allow CdS

deposition. The CdS film on the glass was then annealed at 450 ˚C for 1 h in a furnace (LHT 02/16 LBR, Nabertherm) supplied with pure nitrogen.

The outer ZnS layer was coated following the same CBD procedures. The ZnS coating solution was prepared in an aqueous solution of 0.04 M $Zn(NO_3)_2$ with was chelated with $0.04\times{}^{2}/_{3}$ tri-sodium critate ($Na_3C_6H_5O_7$) mixed with 0.06 M thiourea, and the solution pH was adjusted to 10 [25]. The glass slides with the CdS film were immersed in the solution for ZnS deposition in a water bath at 50 °C for different CBD periods (1, 2, and 3 h). Accordingly, the catalyst films were denoted as CdS/ZnS-1h, CdS/ZnS-2h, and CdS/ZnS-3h for the different ZnS coating periods. The glass slides coated with the catalyst film were then annealed at 450 ˚C for 1 h. The amount of CdS/ZnS coated on the slide surface was calculated by the weight increase after the catalyst coating.

Ruthenium (Ru) was deposited on the surface of the catalyst film by *in-situ* photodeposition in a 10% (vol) acetic acid (CH_3COOH) solution of $RuCl_3$ (Aldrich). The photodeposition was conducted by illuminating (λ>420 nm, 300 W Xe lamp) the CdS/ZnS film for 20 min in 150 mL of the coating solution with a Ru concentration of 53.5 mg/L. For CdS/ZnS-2h, the catalyst layer on the slide weighed about 800 mg. According to the concentration measurement, nearly all Ru^{3+} in the solution (8.025 mg) deposited on the slide after the photodepostion. Thus, the resulting Ru deposition density was approximately 1.0 wt% (i.e. ~8 mg vs. ~800 mg) of the catalyst coating layer of CdS/ZnS-2h. The catalyst film with Ru deposition was denoted as CdS/ZnS/Ru.

2.2 Characterization of the film photocatalysts

The amount (mass) of the film catalyst that was coated on a glass slide was determined from the weight increase after each step of the chemical deposition. The crystalline phase and structural features of the catalysts were analyzed using an X-ray diffraction (XRD)

system (D8 Advance, Burker AXS) with Cu Kα irradiation from 10-90 degrees. The diffuse reflection spectrum (DRS) of the catalyst film was obtained using a UV-vis spectrophotometer (Lambda 25, Perkin Elmer) that was converted from the reflection function to the absorbance function following the Kubelka-Munk method [26]. The morphology of the thin catalyst film was examined under a scanning electron microscope (SEM, Hitachi S-4800 FEG), and the thickness of the catalyst film on the glass surface was measured using an atomic force microscope (AFM, BioMAT™ Workstation).

2.3 Photocatalytic H_2 production with different model organic pollutants under visible light

The photocatalytic hydrogen production experiments were conducted in a cylindrical photo cell made of optical glass. A 300 W Xe lamp setup (PLS-SXE Xe light source, Trustech) was used as the light source with a cutoff filter ($\lambda < 420$ nm) installed to provide visible light (denoted by Vis, light intensity ~ 70 mW/cm^2) and without a cutoff filter to simulate the solar light (denoted by Solar, light intensity ~ 86 mW/cm^2). Two pieces of the glass slides with the catalyst film were placed next to each other in the photo cell filled with 150 mL of water or an organic solution. The light was applied from the top of the photo cell on a total catalyst film area of 27.5 cm^2. Different model organic pollutants (formic acid, methanol, and ethanol) were tested for the photocatalytic H_2 production and organic degradation experiments. The solution had an organic content of 10% by volume and was kept at pH~7. The gas produced during the photo-tests was collected, and its hydrogen and carbon dioxide contents were determined using a gas chromatograph (HP5890 Series II, Hewlett Packard). Each run of the photo-test lasted approximately 4 h. The reactivity of the photocatalyst in different solutions was evaluated in terms of the specific hydrogen

production rate (R) and energy conversion efficiency (η), as determined by the following equations:

$$R_A = \frac{m_{H_2}}{A\,t}, \text{ or} \quad (1)$$

$$R_w = \frac{m_{H_2}}{W\,t}, \text{ and} \quad (2)$$

$$\eta = \frac{R\,\Delta H_C}{I}, \quad (3)$$

where R_A and R_w are the area-based and weight-based specific H_2 production rates, respectively, m_{H2} is the moles of the H_2 produced, t is the duration of the photoreaction, A is the irradiation area (27.5 cm^2), W is the amount (weight) of the catalyst in the photocell for H_2 generation, ΔH_c is the combustion value of H_2 (286 kJ/mol), and I is the light density. The photocatalytic H_2 generation test was repeated 10 times for each catalyst film under an experimental condition to evaluate the reproducibility of the experiment and the stability of the film catalyst. In addition, the amount of Cd^{2+} leaching into the water during the photocatalytic experiments was measured using an atomic absorption spectrometer (AAnalyst 300, Perkin Elmer).

3 Results and Discussion

3.1 Synthesis and optimization of the double-layer film catalysts

The coating solution's pH was found to control the rate of CdS deposition and the quality of the coating layer on glass (Fig. 1). The rate of CdS deposition generally increased as pH increased. As shown by the SEM images, the deposition was slow at pH 8.5 and the surface coating was not completed in 30 min. At pH 9.0, the CdS deposition film was not uniformly distributed on the glass and the coating quality was unsatisfactory. At pH 9.5, the

coating quality greatly improved and a smooth and uniform deposition layer was obtained with a thickness of approximately 150 nm, according to the AFM measurement.

During the coating process, the precursor reaction on the substrate surface leads to heterogeneous precipitation and the resulting film formation on the base substrate. The precipitation of CdS on the glass surface, or $Cd^{2+} + S^{2-} \Leftrightarrow CdS(s)$, was controlled by the concentrations of free Cd^{2+} and S^{2-} in the coating solution. In this study, NH_3 was chosen as the complexing agent for Cd^{2+}, which released a small amount of Cd^{2+} according to the complexion dissociation, i.e. $\left[Cd\left(NH_3\right)_n\right]^{2+} \Leftrightarrow Cd^{2+} + nNH_3$. The NH_3 concentration was related to pH and its equilibrium constant ($K_{NH_3 \cdot H_2O} = 1.79 \times 10^{-5}$). Meanwhile, the free S^{2-} released from hydrolysis of thiourea was also controlled by the solution pH, according to $SC\left(NH_2\right)_2 + OH^- \Leftrightarrow SH^- + CN_2H_2 + H_2O$ and $SH^- + OH^- \Leftrightarrow S^{2-} + H_2O$. At pH 8.5, the hydrolysis of thiourea was slow, which hindered the deposition of CdS on the glass [27]. When the pH was increased to 9.0, the hydrolysis of thiourea became faster. However, due to the low NH_3 level (0.0027 M based on its equilibrium constant), a high concentration of free Cd^{2+} resulted in a rapid CdS precipitation on the glass surface and in the bulk solution. This facilitated a cluster-by-cluster deposition to form a thick and non-uniform coating layer on the glass surface. The coating layer was loose and could easily peel from the surface. At pH 9.5, a smooth and uniform CdS film was formed on the glass with adequate NH_3 (0.0088 M) chelating Cd^{2+} and sufficient hydrolysis of thiourea. The film growth rate and thickness were moderate, for which the heterogeneous 'ion by ion' deposition was expected at the surface with a low potential of film cracking [28].Thus, pH 9.5 was chosen for the deposition of the inner CdS layer.

The ZnS layer was deposited by the similar chelating system at pH 10 to form a condensed film [25]. The ZnS growth rate was controlled by the deposition temperature. The morphology of ZnS and CdS layers and their interface was examined by SEM (Fig. S3,

157 Supporting Material). At a low temperature of 40 ˚C, the ZnS deposited on the CdS surface
158 was thin, uneven and loose, which could easily fall off from the surface. At a high
159 temperature of 60 ˚C, the ZnS film was thick and the interface was loose. At 50 ˚C, the best
160 film deposition quality could be achieved with a compact ZnS layer and its firm adhesion to
161 the inner CdS layer.

162 The outer ZnS layer was found to affect the photo-reactivity of the CdS/ZnS film
163 catalyst. For photocatalytic H_2 production with formic acid as the model organic, hydrogen
164 was produced by the single layer CdS film, and no hydrogen was produced by the single
165 ZnS layer under the visible light and simulated solar light (Fig. 2). Deposition of ZnS on the
166 CdS layer did not reduce its H_2 production activity. On the contrary, the ZnS outer layer
167 significantly increased the H_2 production rate of the photocatalyst film. With the ZnS
168 coating for 2 h, the double-layer film catalyst CdS/ZnS-2h achieved the highest H_2
169 production rate of 31.2 μmol/h under visible light and 45.9 μmol/h under the solar light,
170 which is three times of that obtained with the single-layer CdS film. However, further
171 increasing the ZnS coating period to 3 h resulted in no additional increase of the H_2
172 production rate.

173

174 *3.2 Characterization of the double-layer CdS/ZnS thin film photocatalyst*

175 The inner CdS and outer ZnS layers can be well identified on the glass slides (Fig. 3).
176 The base CdS formed a dense layer on the glass with an average thickness of about 150 nm
177 as measured by the AFM. The outer layer of CdS/ZnS-2h had an average thickness of 125
178 nm consisting of fine ZnS particles. The XRD analysis indicated different crystal phases of
179 the CdS/ZnS film catalyst (Fig. 4). For instance, three XRD peaks at scattering angles (2θ)
180 of 26.5°, 43.8°, and 52.0° could be indexed to the diffractions of the cubic CdS crystal
181 lattice (JCPDS Card No. 75-1546), of which the peaks at 26.5° and 52.0° are associated

with only the cubic phase. The XRD peak at 36.5° is associated with only the hexagonal CdS phase. ZnS crystalline phase appears at 2θ = 28.7º, 48.4º, and 56.4º, which are close to the values reported for cubic ZnS (JCPDS card No. 5-0566).

The diffuse reflection spectra of the single-layer CdS and ZnS films and the double-layer CdS/ZnS film displayed the photo-sensitivity of the catalyst films (Fig. 5). As expected, single-layer ZnS did not responded to visible light. CdS responded well to visible light with a narrow band-gap of 2.23 eV determined from the absorbance edge in Fig. 5. For the double-layer CdS/ZnS film, its absorbance increased greatly in the low wavelength range of visible light in comparison to the single ZnS layer. The ZnS coating on the CdS film also resulted in a slight blue shift of the absorbance edge compared to the single-layer CdS film. The double-layer CdS/ZnS film had a band-gap of 2.45 eV, suggesting a similar response as the CdS film to visible light.

While CdS responses to visible light, ZnS adsorbs only UV irradiation. However, when ZnS was deposited on CdS to form a composite CdS/ZnS thin film, the reactivity of the photocatalyst increased clearly as suggested by the photo-test results. There is an apparent synergistic effect between the two catalyst materials for the photocatalytic process. The use of the more photoreactive CdS layer ensured the reactivity and efficiency of the catalyst film under visible light [24]. Moreover, the sensitive CdS would function as a photo-sensitizer to induce the excitation of ZnS that was in direct contact with CdS. The higher conduction band and lower valence band of ZnS demonstrate the heterojunction of ZnS/CdS. In this case, this heterojunction can establish fast transport channels along with efficient eh separation and effectively suppress the electron loss at the CdS surface. As shown in Fig. S1 (Supplementary Material), the electron flow through the heterojunction between CdS and ZnS is important to the effective electron-hole separation. Similar photoelectrical mechanisms have been identified for quantum-dot sensitized solar cells [29, 30]. Under solar

light, the excited electron of ZnS outer layer injected in to the CB of CdS increased the electron flow to the surface and helped suppress the recombination of electron-hole pairs formed in the CdS inner layer, making the electrons more available for H_2 evolution as show in Fig. S1 [14, 15].

The use of the outer ZnS layer also improved the stability of the CdS-based photocatalyst under either the visible light or simulated solar light. After 10 runs of the photo-H_2 tests, the composite double-layer catalyst retained 90% of its H_2-producing capability under visible light, while the single-layer CdS film retained only 52% of its reactivity for H_2 production (Fig. 6A). A similar comparison of the test results was also observed under the solar light between the photocatalyst films with and without the ZnS layer (Fig. 6B).

The ZnS outer layer also prevented the leaching of Cd^{2+} from the catalyst film during the photocatalytic process. Between test runs 2 and 5, the CdS/ZnS-2h catalyst had an average Cd^{2+} leaching rate of 24.7 µg/h under visible light, while the single-layer CdS film had a Cd^{2+} leaching rate of 73.7 µg/h (Fig. 6A). Between runs 6 and 10, the leaching of Cd^{2+} from CdS/ZnS-2h diminished to a rate of 1.2 µg/h compared to the CdS film with a Cd^{2+} leaching rate of 24.3 µg/h. The similar results were obtained with the same catalyst films under solar light (Fig. 6B). Use of the outer ZnS layer physically separated CdS from the reaction medium to protect the more reactive CdS layer against photo-corrosion.

The adhesion and stability of the coating films are of extremely importance to the performance of the film catalyst. The quality of the catalyst films was regularly assessed by manual examination and visual and SEM observations during the synthesis process and the photocatalytic hydrogen production tests. After a number of test runs, the aqueous solution remained clean and clear, and the SEM images also showed the compact morphology of the films (Fig. S2, Supporting Material). There was no sign of the films peeling off from the slide

surface. The thickness and roughness of the films before and after the hydrogen production tests were also detected by the AFM, and the results presented in Table S1 (Supporting Material) show little changes of the photocatalyst films (the thickness remained at ~150 nm with a roughness of ~13 nm). As reported in Fig. 6, after 10 runs of the photo-H_2 tests, the composite catalyst film retained 90% of its H_2-producing capability under visible light. All of these indicate the good quality and stability of the catalyst films deposited on the glass slides.

3.3 Hydrogen production with simultaneous organic degradation

The CdS/ZnS film catalyst was capable of both photocatalytic H_2 production and organic degradation under visible light and solar light (Fig. 7A). The H_2 production rate increased for the model organic pollutants in an order of ethanol, methanol, and formic acid. For the photocatalyst films in pure water, no hydrogen was produced in the absence of the model organics even under the solar light. The photocatalyst was apparently unable to split water to produce hydrogen under visible light or solar light. However, the presence of organic matters enabled the photocatalyst to produce hydrogen from water. The model organic pollutants function as electron donors for the reduction of H^+ ions, giving rise to H_2 evolution.

Moreover, the Ru deposition on the catalyst surface resulted in a 10-fold increase in H_2 production rate. As Ru possesses a lower Fermi energy level than CdS/ZnS [31], it would function as an electron collector at the surface of the CdS/ZnS film for the electrochemical process. The photo-excited electrons could readily transfer from the photocatalyst to the Ru sites on the catalyst surface. Such an electron collection would facilitate the electron transfer from CdS/ZnS to H^+ ions in the aqueous solution for H_2 evolution. In other words, Ru deposition on the CdS/ZnS surface helps the charge separation on the catalyst, resulting in improved H_2 generation [32].

The highest H_2 production rate under visible light was achieved at 123 mmol/m^2-h with the CdS/ZnS/Ru film in formic acid, with an energy conversion efficiency of 1.41%. The highest H_2 production rate under the simulated solar light was 135 mmol/m^2-h in formic acid, with an energy conversion efficiency of 1.26%. In relation to H^+ reduction for H_2 production, the corresponding organic degradation in terms of the chemical oxygen demand (COD) removal may be estimated using the following formula:

$$COD\ \ removal = \frac{m_{H_2}\ M_{O_2}}{2} \qquad (4)$$

where M_{O2} is the molar mass of O_2 (32 g/mol). The theoretical photocatalytic COD reduction rates for formic acid by the CdS/ZnS/Ru film were 5.4 mg/h in visible light and 6.0 mg/h in solar light (Fig. 7B), corresponding to area-based-specific rates of 1.9 and 2.1 g COD/m^2-h, respectively. Degradation of formic acid resulted in CO_2 production. During the photocatalytic test, CO_2 was generated at a rate of 73 mmol/m^2-h in the gaseous phase, which agrees well with the theoretical COD reduction rate of formic acid. The molar ratio of H_2 to CO_2 produced was approximately 1:1, suggesting a complete decomposition of formic acid. It is believed that formic acid ($E^0_{CO2/HCOOH}$ = -0.126 V) functioned as an electron donor to trap photo-generated holes on the valence band of CdS/ZnS [33], resulting in the organic decomposition and CO_2 production.

The hydrogen production rates in the methanol and ethanol solutions under visible light were 104 and 92 mmol/m^2-h, respectively, which are higher than that reported by Daskalaki et al. [34] for the Pt/CdS/TiO_2 film catalyst. Hydrogen production from 10% ethanol achieved an energy conversion efficiency of 1.04% in visible light, which is also higher than the efficiency reported by [35] for the Pt/TiO_2 film catalyst in 80% ethanol under UV irradiation. Nonetheless, CO_2 production was not detected during the photocatalytic H_2 generation in both methanol and ethanol solutions. It is apparent that the photocatalytic reactions resulted in organic destruction and intermediate formation other than complete

organic mineralization [14, 36]. When the CdS/ZnS film catalyst was excited in visible light, the photo-generated holes would attack methanol and ethanol to produce methanal and ethanal, respectively, according to the following reactions [14, 37]:

$$CH_3OH + h^+ \longrightarrow HCHO + H^+;$$

$$CH_3CH_2OH + h^+ \longrightarrow CH_3CHO + H^+.$$

The composite CdS/ZnS double-layer film structure exhibited a synergetic function of the catalyst materials for photocatalytic H_2 generation and organic degradation. Moreover, as described previously, film-type photocatalysts can be easily separated from water or solutions for repeated use. This property is particularly important in wastewater treatment applications. The catalyst film also allows better light penetration compared with the suspension of catalyst powders [38]. The CdS/ZnS/Ru film catalyst had a weight-based-specific H_2 production rate of up to 8.5 mmol/g-h for visible light irradiation, which was higher than that of the CdS/ZnS/Ru catalyst powders. This implies that the photocatalyst film is as good as catalyst powders in utilizing visible light or solar light for H_2 production. Together with its immobilized feature, the multilayer CdS/ZnS/Ru film catalyst demonstrates a great more potential for simultaneous photocatalytic H_2 production and wastewater organic degradation.

4 Conclusions

- The double-layer CdS/ZnS film catalyst was synthesized by chemical bath deposition for photocatalytic H_2 production under visible light. The ZnS outer layer helps suppress the recombination of photo-generated electron-hole pairs on the more photosensitive CdS base layer, leading to a faster H_2 production rate. Moreover, compared with the single-layer CdS film, the use of ZnS in the double-layer CdS/ZnS film greatly

improved the stability of the catalyst and prevented the leaching of Cd^{2+} from the catalyst film.

- The visible light-driven photocatalyst was capable of both producing hydrogen and degrading model organic pollutants (formic acid, methanol, and ethanol). The CdS/ZnS/Ru film had an H_2 production rate of 123 mmol/m^2-h in the formic acid solution with an energy conversion efficiency of 1.41%. In relation to H_2 production, the theoretical COD reduction rate for formic acid was 1.9 g COD/m^2-h by the catalyst film under visible light.
- As the multilayer CdS/ZnS/Ru catalyst film is well immobilized and can be easily separated from water, it presents a great potential in both photocatalytic H_2 generation and organic wastewater treatment using solar energy.

Acknowledgments

This research was supported by grants HKU714112E from the Research Grants Council (RGC) and SEG_HKU10 from the University Grants Committee (UGC) of the Government of Hong Kong SAR, and #51308230 from the National Natural Science Foundation of China (NSFC). The technical assistance of Mr. Keith C.H. Wong is highly appreciated.

References:

[1] K. Maeda, K. Teramura, D.L. Lu, T. Takata, N. Saito, Y. Inoue, K. Domen, Photocatalyst releasing hydrogen from water - enhancing catalytic performance holds promise for hydrogen production by water splitting in sunlight., Nature 440 (2006) 295.

[2] C. Grimes, O.K. Varghese, S. Ranjan, Light, water, hydrogen: the solar generation of hydrogen by water photoelectrolysis, Springer, New York, USA, 2008.

[3] P. Lianos, Production of electricity and hydrogen by photocatalytic degradation of organic wastes in a photoelectrochemical cell: The concept of the Photofuelcell: A review of a re-emerging research field, J. Hazard. Mater. 185 (2011) 575-590.

[4] M.T. Lee, M. Werhahn, D.J. Hwang, N. Hotz, R. Greif, D. Poulikakos, C.P. Grigoropoulos, Hydrogen production with a solar steam-methanol reformer and colloid nanocatalyst, Int. J. Hydrogen Energy 35 (2010) 118-126.

[5] M. Law, L.E. Greene, A. Radenovic, T. Kuykendall, J. Liphardt, P.D. Yang, ZnO-Al_2O_3 and ZnO-TiO_2 core-shell nanowire dye-sensitized solar cells, J. Phys. Chem. B 110 (2006) 22652-22663.

[6] X. Zong, H.J. Yan, G.P. Wu, G.J. Ma, F.Y. Wen, L. Wang, C. Li, Enhancement of photocatalytic H_2 evolution on CdS by loading MoS_2 as cocatalyst under visible light irradiation, J. Am. Chem. Soc. 130 (2008) 7176-7177.

[7] H. Yan, J. Yang, G. Ma, G. Wu, X. Zong, Z. Lei, J. Shi, C. Li, Visible-light-driven hydrogen production with extremely high quantum efficiency on Pt-PdS/CdS photocatalyst, J. Catal. 266 (2009) 165-168.

[8] A. Patsoura, D.I. Kondarides, X.E. Verykios, Photocatalytic degradation of organic pollutants with simultaneous production of hydrogen, Catal. Today 124 (2007) 94-102.

[9] Y.J. Zhang, L. Zhang, Preparation of Ru-loaded CdS/Al-HMS nanocomposites and production of hydrogen by photocatalytic degradation of formic acid, Appl. Surf. Sci. 255 (2009) 4863-4866.

[10] H. Park, A. Bak, Y.Y. Ahn, J. Choi, M.R. Hoffmannn, Photoelectrochemical performance of multi-layered BiOx-TiO2/Ti electrodes for degradation of phenol and production of molecular hydrogen in water, J. Hazard. Mater. 211 (2012) 47-54.

[11] N.L. Wu, M.S. Lee, Z.J. Pon, J.Z. Hsu, Effect of calcination atmosphere on TiO_2 photocatalysis in hydrogen production from methanol/water solution, J. Photochem. Photobiol. B: Chem. 163 (2004) 277-280.

[12] M. Zalas, M. Laniecki, Photocatalytic hydrogen generation over lanthanides-doped titania, Sol. Energy Mater. Sol. Cells 89 (2005) 287-296.

[13] S.M. Ji, P.H. Borse, H.G. Kim, D.W. Hwang, J.S. Jang, S.W. Bae, J.S. Lee, Photocatalytic hydrogen production from water-methanol mixtures using N-doped $Sr_2Nb_2O_7$ under visible light irradiation: effects of catalyst structure, Phys. Chem. Chem. Phys. 7 (2005) 1315-1321.

[14] J.P. Best, D.E. Dunstan, Nanotechnology for photolytic hydrogen production: colloidal anodic oxidation, Int. J. Hydrogen Energy 34 (2009) 7562-7578.

[15] Y.W. Cao, U. Banin, Growth and properties of semiconductor core/shell nanocrystals with InAs cores, J. Am. Chem. Soc. 122 (2000) 9692-9702.

[16] X.J. Zheng, L.F. Wei, Z.H. Zhang, Q.J. Jiang, Y.J. Wei, B. Xie, M.B. Wei, Research on photocatalytic H_2 production from acetic acid solution by Pt/TiO_2 nanoparticles under UV irradiation, Int. J. Hydrogen Energy 34 (2009) 9033-9041.

[17] C. Guillard, B. Beaugiraud, C. Dutriez, J.M. Herrmann, H. Jaffrezic, N. Jaffrezic-Renault, M. Lacroix, Physicochemical properties and photocatalytic activities of TiO_2 films prepared by sol-gel methods, Appl. Catal. B: Env. 39 (2002) 331-342.

[18] S. Zhou, A.K. Ray, Kinetic studies for photocatalytic degradation of eosin B on a thin film of titanium dioxide, Ind. Eng. Chem. Res. 42 (2003) 6020-6033.

[19] G. Balasubramanian, D.D. Dionysiou, M.T. Suidan, I. Baudin, J.M. Laîné, Evaluating the activities of immobilized TiO_2 powder films for the photocatalytic degradation of organic contaminants in water, Appl. Catal. B: Env. 47 (2004) 73-84.

[20] K.L. Rosas-Barrera, J.A. Pedraza-Avella, B.P. Ballén-Gaitán, J. Cortés-Peña, J.E. Pedraza-Rosas, D.A. Laverde-Cataño, Photoelectrolytic hydrogen production using Bi_2MNbO_7 (M=Al, Ga) semiconductor film electrodes prepared by dip-coating, Mater. Sci. Eng. B 176 (2011) 1359-1363.

[21] D.G. Diso, G.E.A. Muftah, V. Patel, I.M. Dharmadasa, Growth of CdS layers to develop all-electrodeposited CdS/CdTe thin-film solar cells, J. Electrochem. Soc. 157 (2010) H647-H651.

[22] N. Strataki, P. Lianos, Optimization of parameters for hydrogen production by photocatalytic alcohol reforming in the presence of Pt/TiO_2 nanocrystalline thin films, J. Adv. Oxid. Technol. 11 (2008) 111-115.

[23] S. Chun, K.S. Han, J.S. Lee, H.J. Lim, H. Lee, D. Kim, Fabrication CdS thin film and nanostructure grown on transparent ITO electrode for solar cells, Curr. Appl. Phys. 10 (2010) S196-S200.

[24] X. Wang, K. Shih, X.Y. Li, Photocatalytic hydrogen generation from water under visible light using core/shell nano-catalysts, Water Sci. Technol. 61 (2010) 2303-2308.

[25] A. Cheng, D.B. Fan, H. Wang, B.W. Liu, Y.C. Zhang, H. Yan, Chemical bath deposition of crystalline ZnS thin films, Semicond. Sci. Technol. 18 (2003) 676-679.

[26] P. Kubelka, F. Munk, Ein Beitrag zur Optik der Far- banstriche, Zeitschrift Technische Physik 12 (1931) 593-601.

[27] Q. Liu, G.B. Mao, Comparison of CdS and ZnS thin films prepared by chemical bathd deposition, Surf. Rev. Lett. 16 (2009) 469-474.

[28] T. Ye, Z. Suo, A.G. Evans, Thin-Film Cracking and the Roles of Substrate and Interface, International Journal of Solids and Structures 29 (1992) 2639-2648.

[29] G. Hodes, Comparison of Dye- and Semiconductor-Sensitized Porous Nanocrystalline Liquid Junction Solar Cells, The Journal of Physical Chemistry C 112 (2008) 17778-17787.

[30] S.W. Jung, J.-H. Kim, H. Kim, C.-J. Choi, K.-S. Ahn, ZnS overlayer on in situ chemical bath deposited CdS quantum dot-assembled TiO2 films for quantum dot-sensitized solar cells, Curr. Appl. Phys. 12 (2012) 1459-1464.

[31] A. Kudo, M. Sekizawa, Photocatalytic H_2 evolution under visible light irradiation on Ni-doped ZnS photocatalyst, Chem. Commun. (2000) 1371-1372.

[32] R. Dholam, N. Patel, A. Miotello, Efficient H_2 production by water-splitting using indium-tin-oxide/V-doped TiO_2 multilayer thin film photocatalyst, Int. J. Hydrogen Energy 36 (2011) 6519-6528.

411 [33] T. Chen, G. Wu, Z. Feng, G. Hu, W. Su, P. Ying, C. Li, In situ FT-IR study of
412 photocatalytic decomposition of formic acid to hydrogen on Pt/TiO_2 catalyst, Chinese J.
413 Catal. 29 (2008) 105-107.
414 [34] V.M. Daskalaki, M. Antoniadou, G.L. Puma, D.I. Kondarides, P. Lianos, Solar
415 light-responsive $Pt/CdS/TiO_2$ photocatalysts for hydrogen production and simultaneous
416 degradation of inorganic or organic sacrificial agents in wastewater, Environ. Sci.
417 Technol. 44 (2010) 7200-7205.
418 [35] N. Strataki, V. Bekiari, D.I. Kondarides, P. Lianos, Hydrogen production by
419 photocatalytic alcohol reforming employing highly efficient nanocrystalline titania
420 films, Appl. Catal. B: Env. 77 (2007) 184-189.
421 [36] Y. Lin, R.F. Lin, F. Yin, X.R. Xiao, M. Wu, W.Z. Gu, W.Z. Li, Photoelectrochemical
422 studies of H_2 evolution in aqueous methanol solution photocatalysed by Q-ZnS
423 particles, J. Photochem. Photobiol. B: Chem. 125 (1999) 135-138.
424 [37] G.L. Chiarello, L. Forni, E. Selli, Photocatalytic hydrogen production by liquid- and
425 gas-phase reforming of CH_3OH over flame-made TiO_2 and Au/TiO_2, Catal. Today 144
426 (2009) 69-74.
427 [38] M. Fathinia, A.R. Khataee, M. Zarei, S. Aber, Comparative photocatalytic degradation
428 of two dyes on immobilized TiO_2 nanoparticles: Effect of dye molecular structure and
429 response surface approach, J. Mol. Catal. A: Chem. 333 (2010) 73-84.
430
431

Figure captions:

Fig. 1. SEM micrographs of the CdS catalyst film deposited at (A) pH = 8.5, (B) pH = 9.0, and (C) pH = 9.5 (left: cross-section; right: surface).

Fig. 2. Photocatalytic H_2 production under visible light or simulated solar light by the catalyst films with different amounts of ZnS deposition. (ZnS-1h, ZnS-2h, and ZnS-3h specify the duration (1, 2, and 3 h) of ZnS deposition on the catalyst films)

Fig. 3. SEM images of the double-layer CdS/ZnS thin film on glass (top: cross-section; bottom, surface).

Fig. 4. XRD patterns of the CdS and the CdS/ZnS catalyst films (CdS-black square, ZnS-open square).

Fig. 5. Diffuse reflection spectra of the double-layer CdS/ZnS film and the single-layer CdS and ZnS films.

Fig. 6. Comparisons between the double-layer CdS/ZnS catalyst film and the single-layer CdS film in terms of H_2 production, the stability of the photocatalytic reactivity, and the rate of Cd^{2+} release under (A) visible light and (B) simulated solar light (each test lasted 4 h).

Fig. 7. (A) Photocatalytic H_2 production and (B) the corresponding COD removal rate by the CdS/ZnS and CdS/ZnS/Ru catalyst films in different organic solutions.

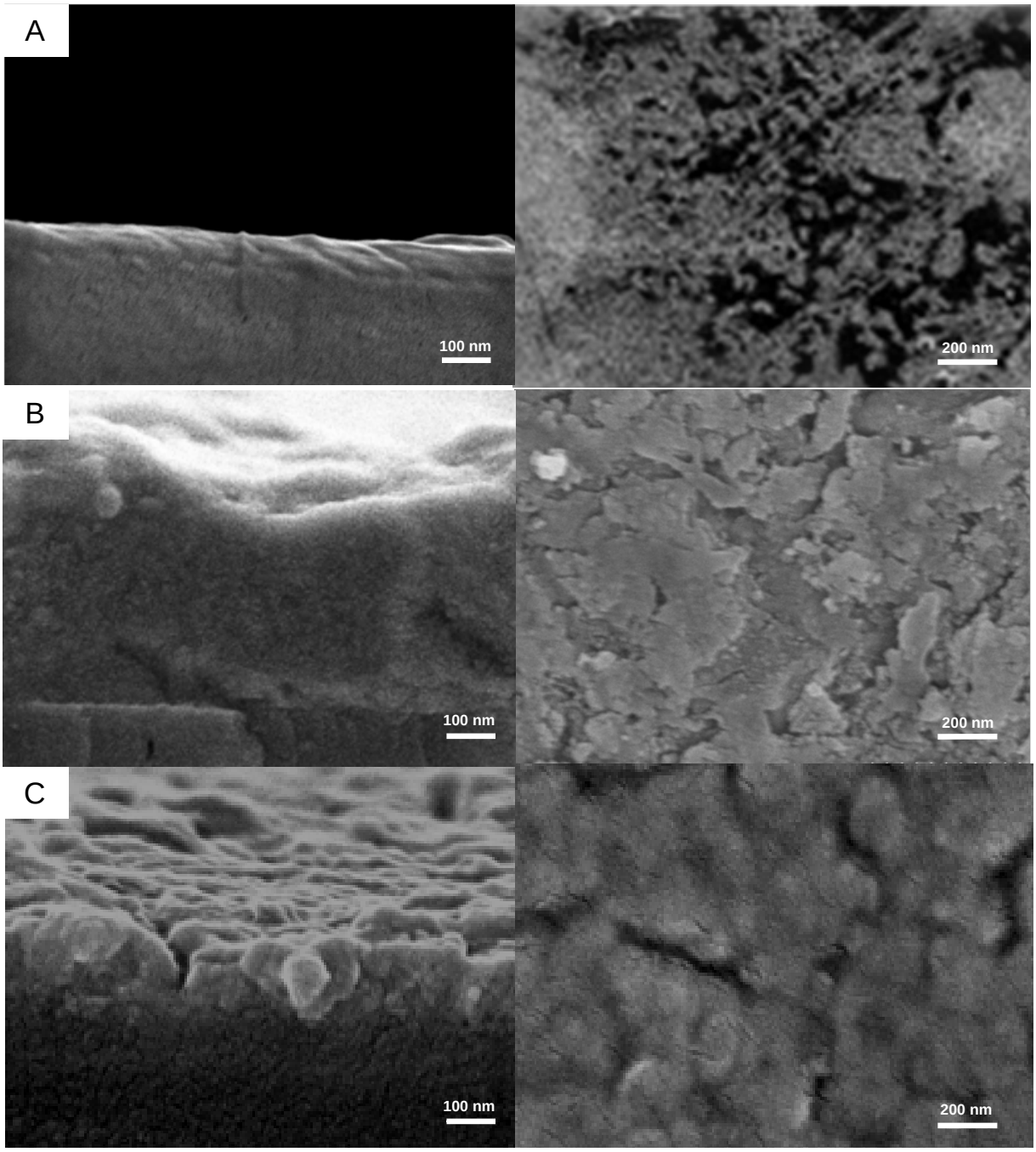

Fig. 1. SEM micrographs of the CdS catalyst film deposited at (A) pH = 8.5, (B) pH = 9.0, and (C) pH = 9.5 (left: cross-section; right: surface).

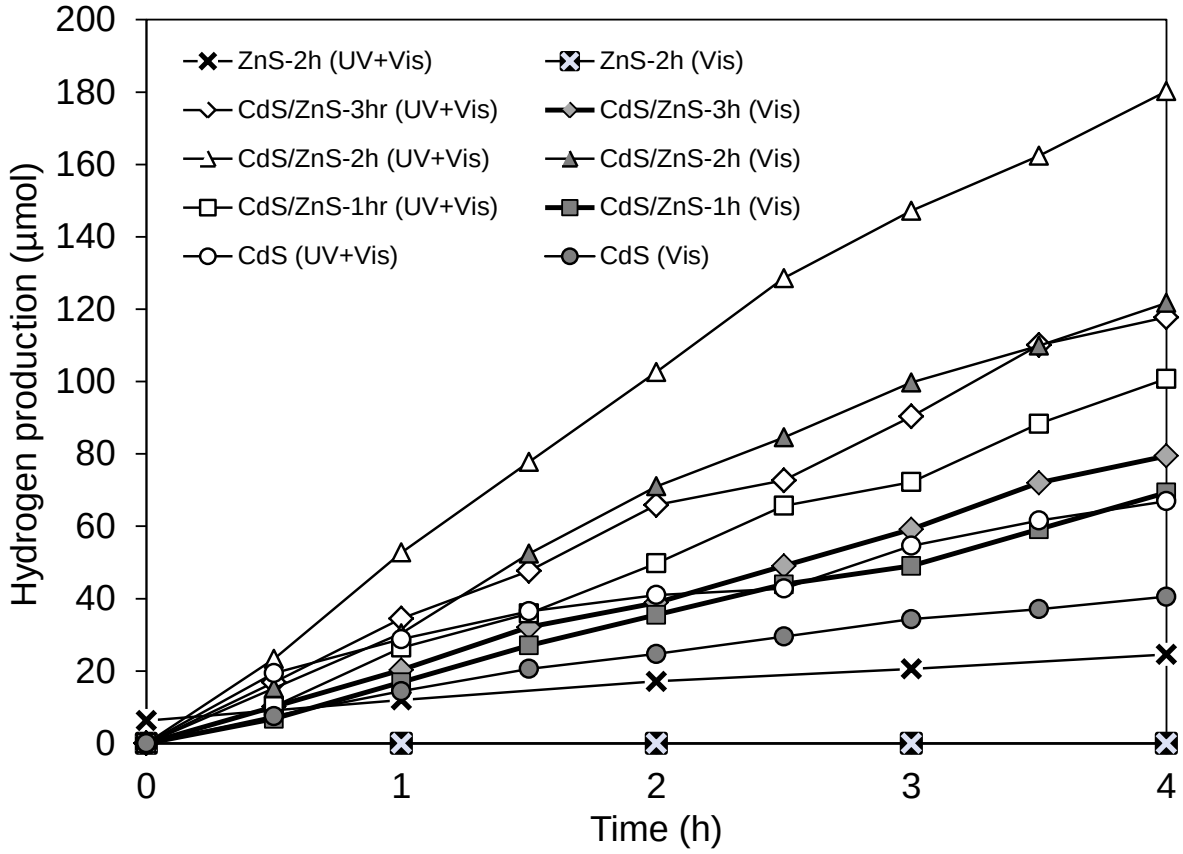

Fig. 2. Photocatalytic H_2 production under visible light or simulated solar light by the catalyst films with different amounts of ZnS deposition. (ZnS-1h, ZnS-2h, and ZnS-3h specify the duration (1, 2, and 3 h) of ZnS deposition on the catalyst films)

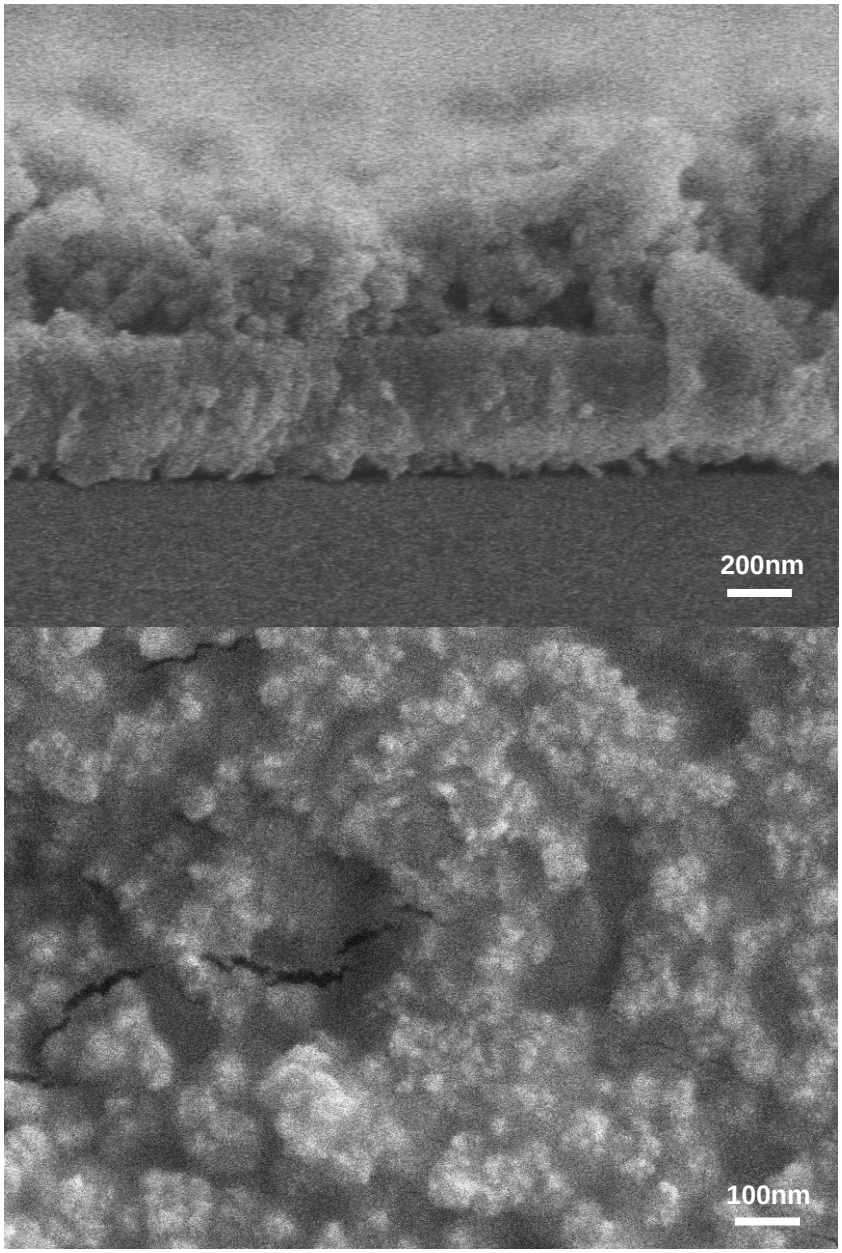

Fig. 3. SEM images of the double-layer CdS/ZnS thin film on glass (top: cross-section; bottom, surface).

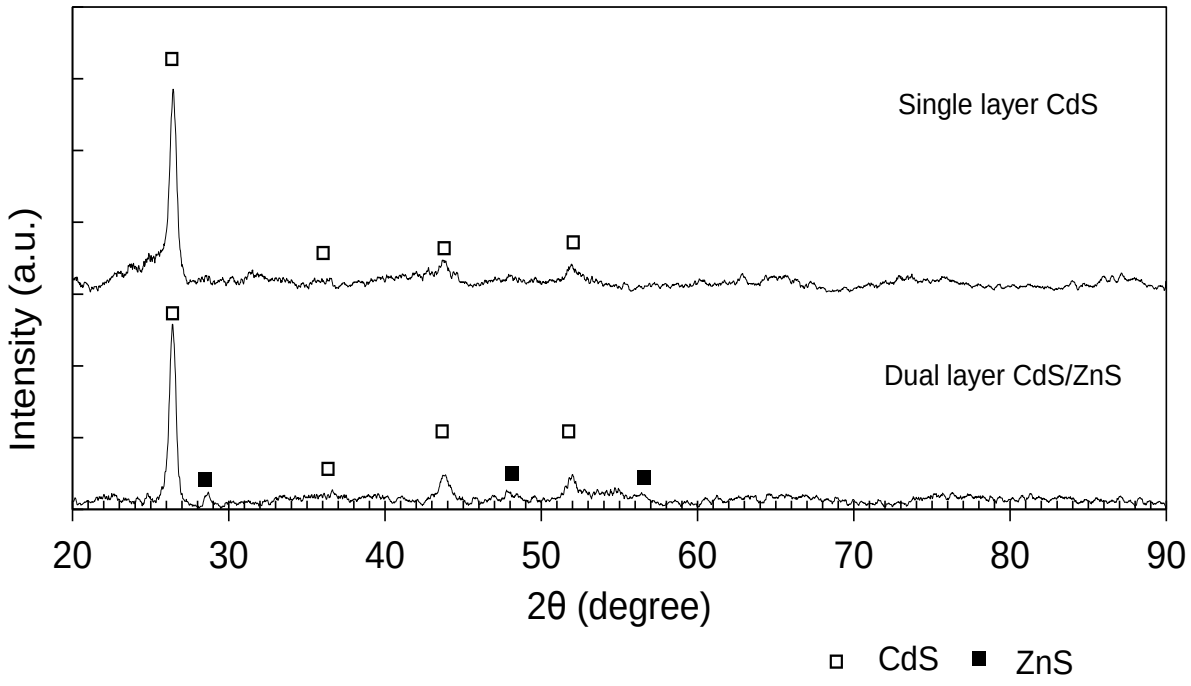

Fig. 4. XRD patterns of the CdS and the CdS/ZnS catalyst films (CdS-black square, ZnS-open square).

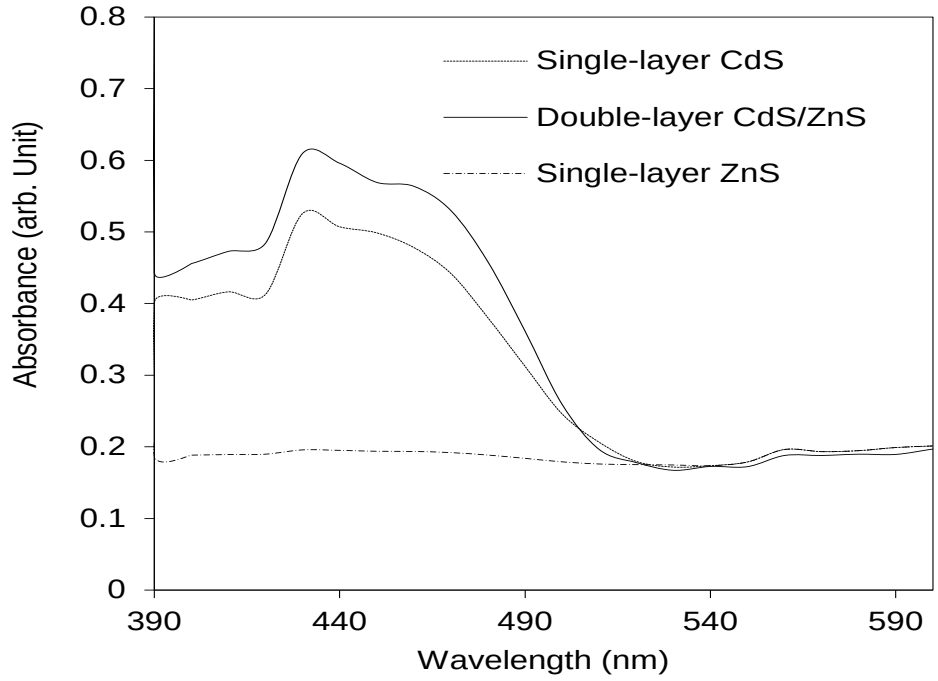

Fig. 5. Diffuse reflection spectra of the double-layer CdS/ZnS film and the single-layer CdS and ZnS films.

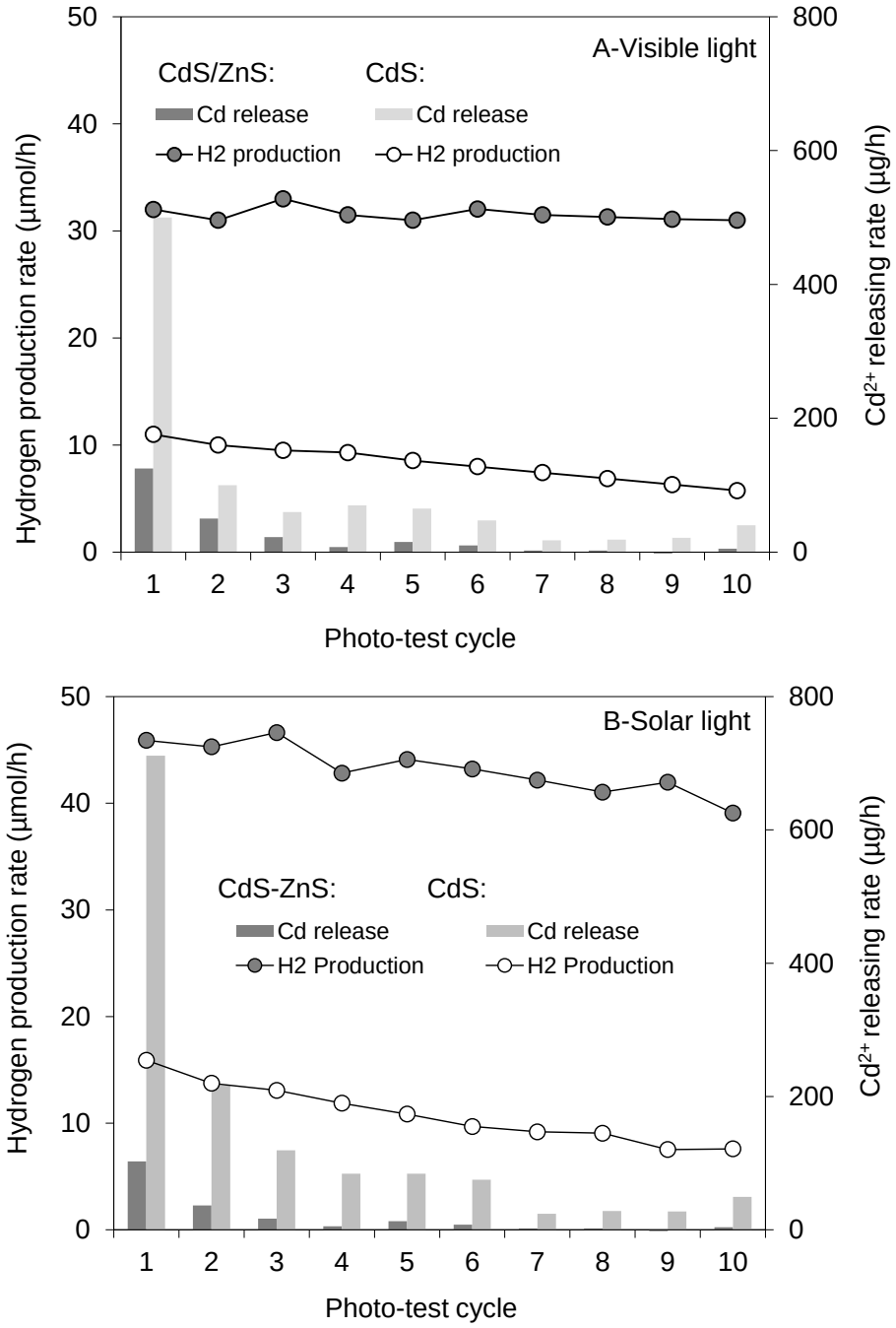

Fig. 6. Comparisons between the double-layer CdS/ZnS catalyst film and the single-layer CdS film in terms of H_2 production, the stability of the photocatalytic reactivity, and the rate of Cd^{2+} release under (A) visible light and (B) simulated solar light (each test lasted 4 h).

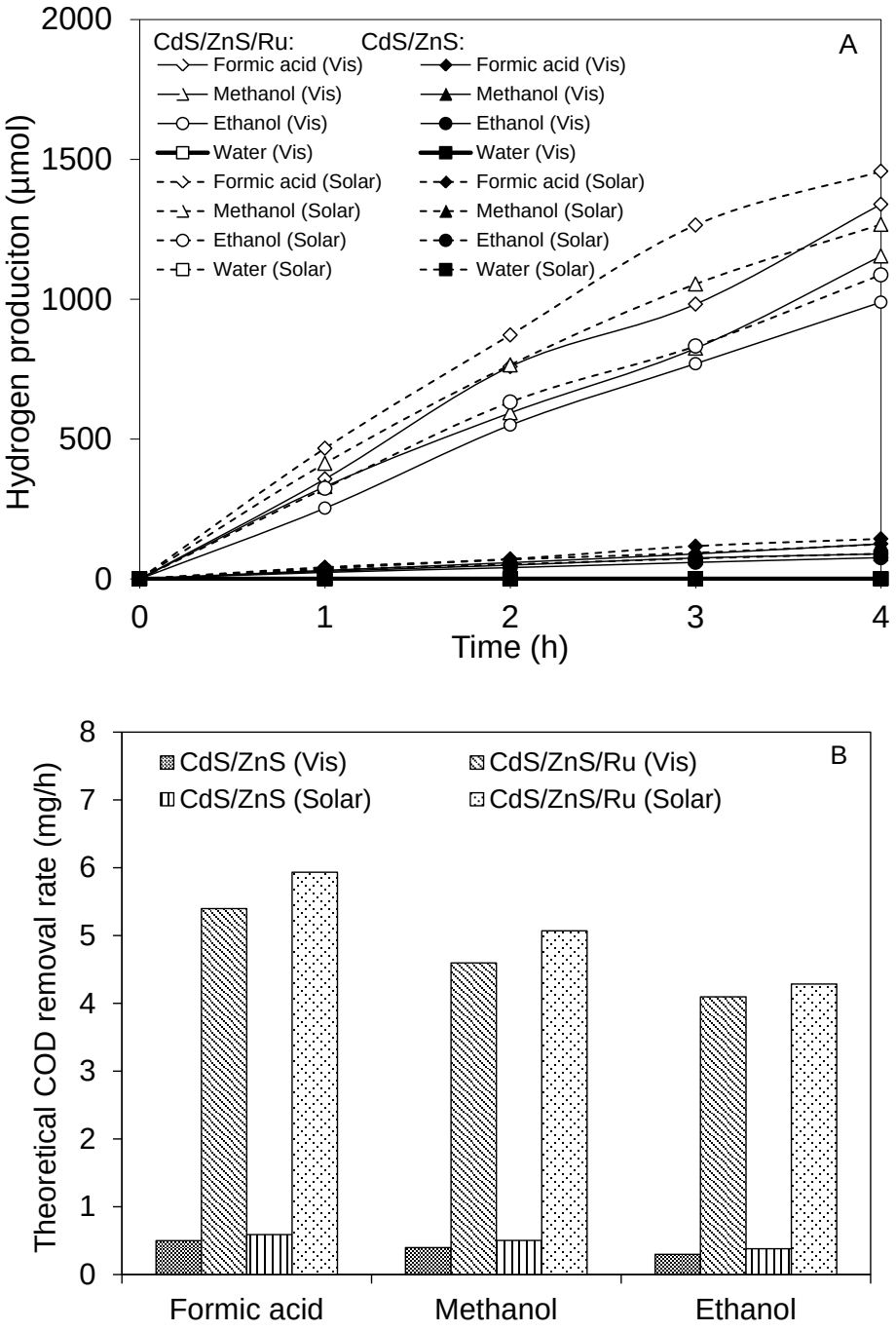

Fig. 7. (A) Photocatalytic H_2 production and (B) the corresponding COD removal rate by the CdS/ZnS and CdS/ZnS/Ru catalyst films in different organic solutions.

Supporting Material

Photocatalytic hydrogen generation with simultaneous organic degradation by a visible light-driven CdS/ZnS film catalyst

Xi Wang[1,2] and Xiao-yan Li[2]*

1 School of Chemistry and Environment, South China Normal University, Guangzhou, Guangdong, China

2 Environmental Engineering Research Centre, Department of Civil Engineering, The University of Hong Kong, Pokfulam Road, Hong Kong

(*Corresponding author: phone: 852 2859-2659; fax: 852 2859-5337; e-mail: xlia@hkucc.hku.hk)

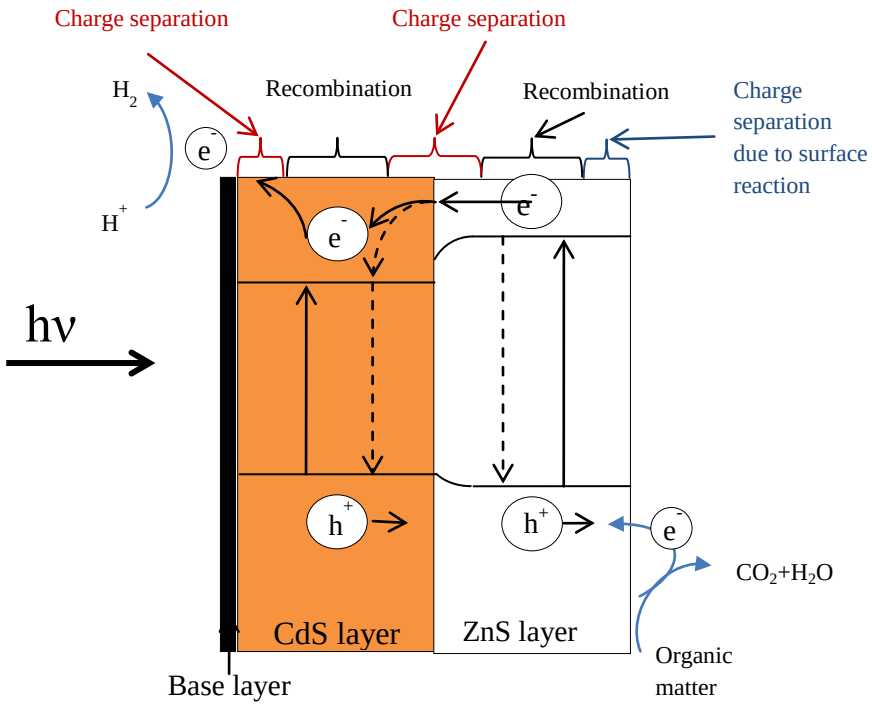

Fig. S1. Illustration of the synergistic effect of two-layer CdS/ZnS on photo-induced electron transfer and the resulting hydrogen evolution and organic degradation. (e^- and h^+ signify photo-induced electron and hole, respectively)

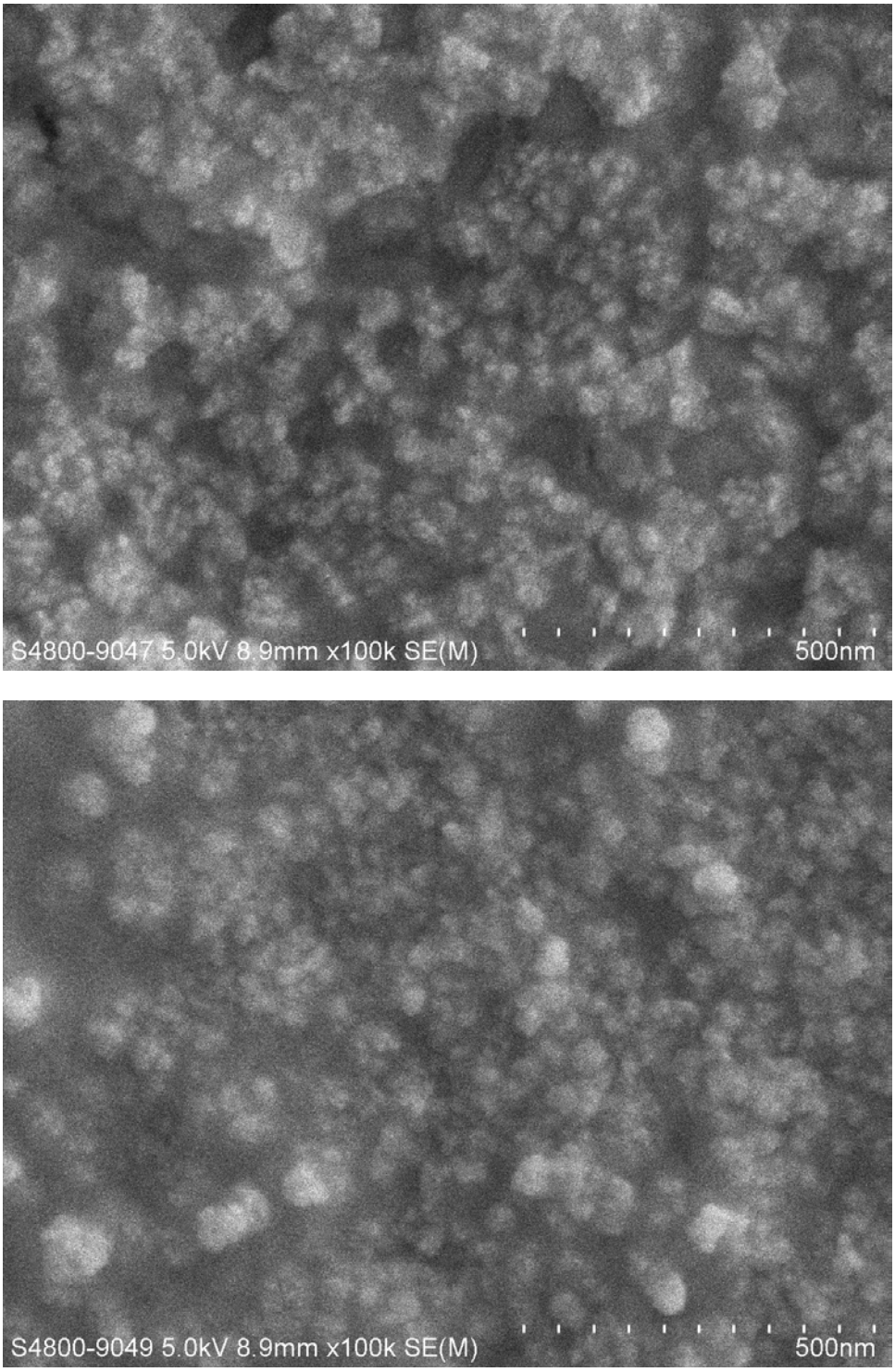

Fig. S2. SEM images of the CdS/ZnS thin film coated on the glass slide before (top) and after (bottom) the photocatalytic hydrogen production test.

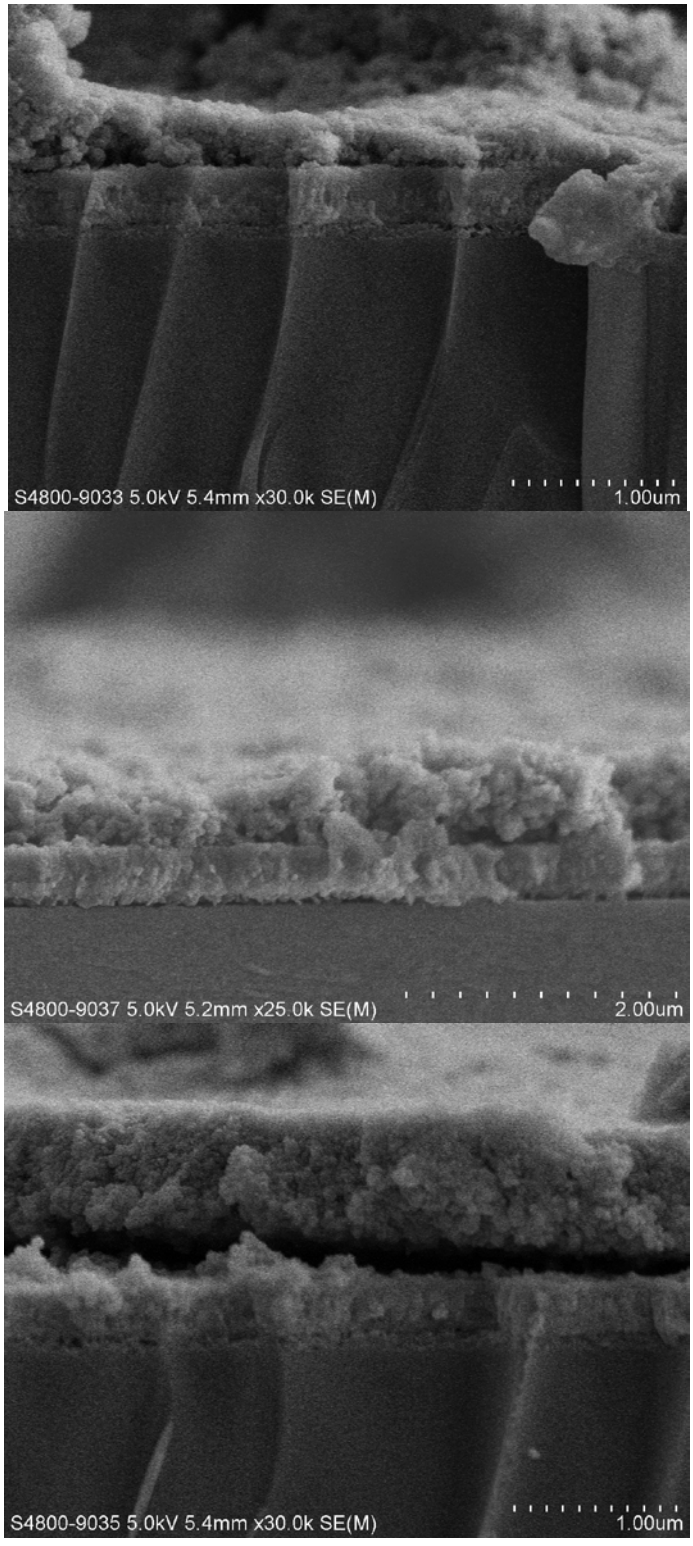

Fig. S3. SEM images of the ZnS layer deposited on the surface of the CdS layer on the glass at different deposition temperatures (top: 40 ˚C, middle: 50 ˚C, and bottom: 60 ˚C).

Table S1. The thickness and roughness of the double-layer CdS/ZnS thin film on glass detected by the AFM before and after the photocatalytic hydrogen production tests.

	Thickness (nm)	Roughness (nm)
Before photo-test	150±7	12.9±2.1
After photo-test	148±8	13.3±1.6